

# Predicting gearbox bearing failure

Gearboxes for rolling mills are complex machines and their reliability is crucial. Condition monitoring systems are useful tools for estimating defects on main gearbox components, but their performance relies upon the training procedure, which often requires a very expensive and experimental set-up. This paper introduces a numerical approach to predict the effects of bearing failure under several working conditions. The generated outputs correspond to different fault conditions and will constitute a useful database to tune up and train the entire apparatus of the condition monitoring system (CMS) of rolling mill gearboxes. By **S.Cinquemani<sup>1</sup>**, **F.Rosa<sup>1</sup>**, **E. Osto<sup>2</sup>**

GEARBOXES for rolling mills are complex machines that cannot be treated as commodities; they are part of a complex drive system that, in case of failure, can seriously affect plant productivity. [1], [2], [3].

From this perspective, early detection of improper operating conditions, as provided by condition monitoring systems (CMS), is a chance to plan extraordinary maintenance to prevent sudden interruptions and identify primary rather than secondary causes of failure. [4], [5], [6]. It is worth mentioning that preventive maintenance implies negligible costs compared to those related to secondary failure causes, such as bearing replacement versus gear and shaft replacement.

In fact, bearings represent a typical source of gearbox failure or improper operation. [7], [8], [9]. Gradual deterioration of operating behaviour is normally the

first sign of bearing damage. Depending on the operating conditions, a few weeks, or even a few months, may pass from the time damage begins to the moment when the bearing actually fails because of contact fatigue damaging mechanisms. This typical progressive damage evolution makes bearings especially suitable for continuous condition monitoring analysis.

From the perspective of failure detection, bearing damage results when there is an increase in operating temperature, lubricant contamination and vibration. In principle, all these parameters can be measured by CMS, but the techniques based on the analysis of vibration signals are the most efficient, as they can provide an earlier identification of the specific bearing involved and can give more information on the kind of damage.

Usually, to properly set up the algorithm, measures associated both with standard operating conditions and malfunctioning are used. This paper investigates the possibility of training a CMS by exploiting numerical analysis based on models of the machine under several operating conditions [10], [11]. This approach would avoid the need for expensive experimental tests and quantitative estimations of bearing damage.

## Mathematical model

An outline of a rolling mill can be seen in **Fig. 1**. Hot steel is rolled through a sequence of rolling stands or – with reversible mills – in multiple runs between the stand's rolling rolls. At each run, the rolled section is reduced and the bar elongated.

To generate “virtual accelerations”

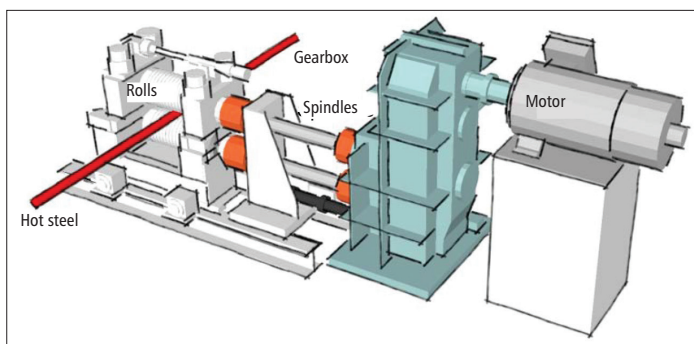


Fig 1. Outline of a rolling mill

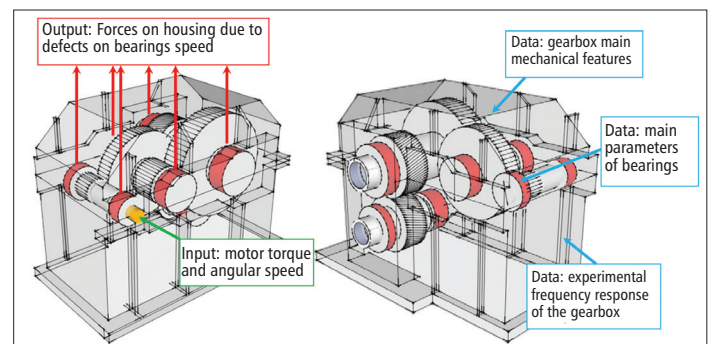


Fig 2. Graphical representation of the mathematical model

1- Department of Mechanical Engineering, Politecnico di Milano, Via La Masa 1, 20156, Milan, Italy  
2- Primetals Technologies Italy, Via Pomini 92, Marnate, Italy

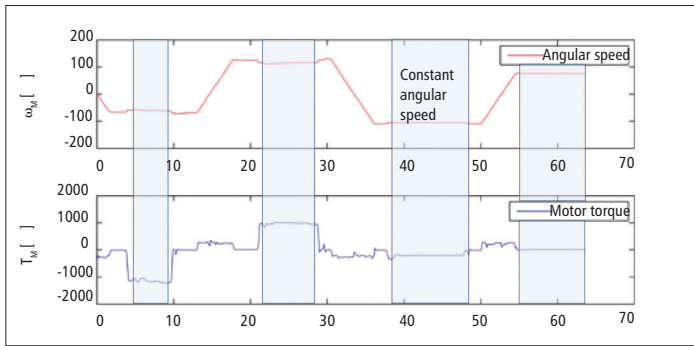


Fig 3. Experimental data (motor torque and motor angular speed)

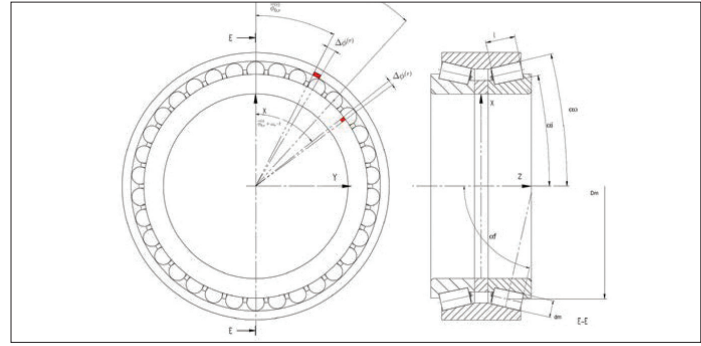


Fig 4. Bearing reference system and race defects definition

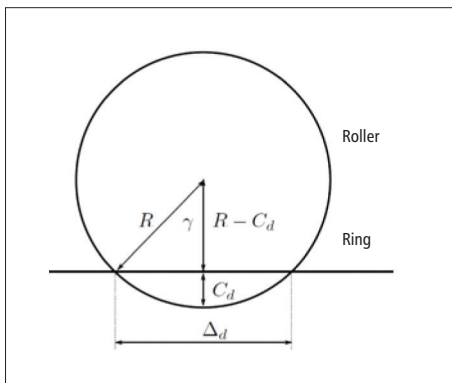


Fig 5. (Left) Geometrical relationship between the depth ( $C_d$ ) and the width ( $\Delta_d$ ) of the defect

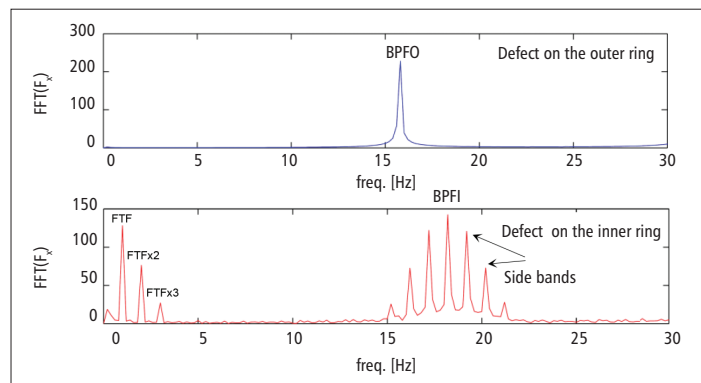


Fig 6. (Right) Spectra of accelerations measured close to a damaged bearing (up – defect on the outer ring, bottom – defect on the inner ring)

related to bearing malfunction in the gearbox, a mathematical model of the system has to be developed. A 'lumped parameter' model has been conceived and deployed for rolling mill gearboxes (Fig. 2). It takes into account the main mechanical and geometrical features, main gear parameters and the most important information on the bearings involved.

First the model needs to input the torque ( $T_M$ ) and angular speed ( $\omega_M$ ) of the motor. This information is collected from the field (Fig. 3) and is limited to conditions in which the speed is constant. Then the kinetostatic model of the transmission calculates the forces on bearings along the three main directions X, Y, Z and the corresponding displacement of the shaft along the same directions ( $\Delta x$ ,  $\Delta y$ ,  $\Delta z$ ) with respect to the housing.

Bearing defects, like pits on any race, periodically change the stiffness of the bearing itself and how it transfers the forces from the shaft to the housing.

For generic roller bearings, the development of the relationship between load and displacement is based on the following key steps (symbols and conventions are illustrated in Fig. 4 for a double row tapered roller bearing, but can be easily extended to all the

bearings):-

1. Define an arbitrary position for each roller.
2. Assign a displacement to the inner ring ( $\Delta x$ ,  $\Delta y$ ,  $\Delta z$ ) as obtained by loads on the bearing
3. Determine overall contact deformation of a generic roller due to these inner ring displacements.
4. Define a relationship between this deformation and the corresponding load (Hertz Theory).
5. Determine how this load is 'distributed' among contacting surfaces on the basis of equilibrium equations.
6. Determine the forces acting on each race as resultant of the forces exerted on it by each roller.

Even though more sophisticated models of bearing internal load distribution can be found in literature (see, for example, <sup>[12]</sup>), a simplified calculation approach has been adopted in this model, to have affordable computational time.

**Bearing defect's fingerprint**

According to different operating conditions (ie. load and angular speed) each bearing has a distinctive behaviour during malfunctioning that can be used as a fingerprint to detect damages.

**Cage wear model**

Cage wear was introduced by assuming that its effect on the bearing global model? can be considered by changing the circumferential positions (with respect of their evenly spaced theoretical positions) of the rollers with respect to the rings. From a mathematical perspective, after having defined the maximum circumferential displacement ( $\epsilon WC$ ) of the rollers, there is a need to define the distribution of these displacements in order to locate all of them. If this type of defect is introduced, it implies that the rollers are no longer evenly spaced, as assumed in the model of a healthy bearing.

**Race pit model**

Reducing the contact deformation of a roller when it is 'on the blocks' simulates the presence of a pit stop in a race. This condition leads to a reduction of the load that can be transmitted by a simple roller/ball. A regular function  $C_d$  is used to describe a generic irregularity of a race (i.e. any deviation from its nominal shape measured along the normal direction). To reduce the number of variables, a simple relationship between the depth ( $C_d$ ) and the width ( $\Delta_d$ ) of the defect has been imposed as shown in Fig. 5. To evaluate the effects of bearing damage,

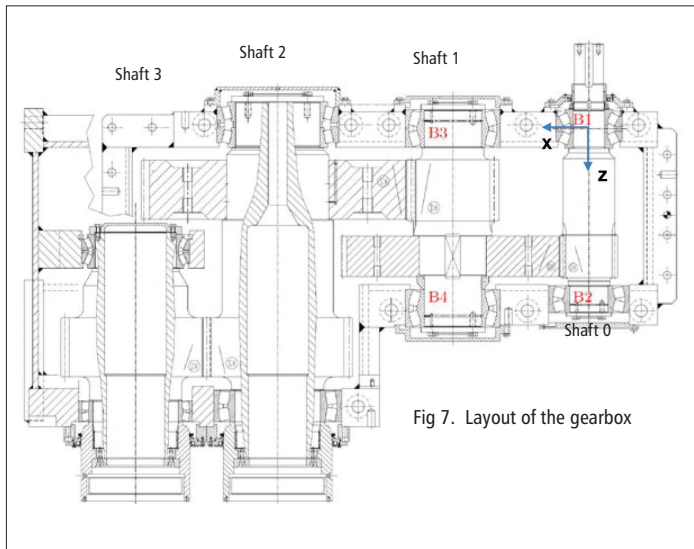


Fig 7. Layout of the gearbox

B1	Tapered roller	SKF 31326
B2	Spherical	SKF 22332
B3	Spherical	SKF 24148
B4	Spherical	SKF 24148

Table 1. Configuration of bearings

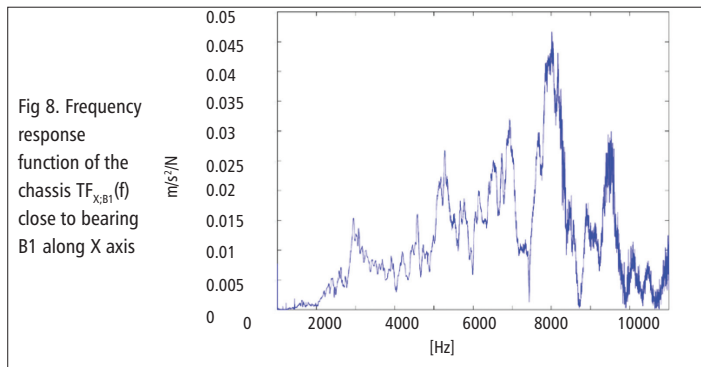


Fig 8. Frequency response function of the chassis  $TF_{x,B1}(f)$  close to bearing B1 along X axis

it is possible to set different values of  $C_d$ , and  $\Delta d$ .

For each roller, the algorithm evaluates the corresponding deformation due to the displacement of the inner ring and the corresponding transmitted force. When a roller is over a defect, its deformation decreases as the load it is transmitting. By considering all the rollers it is then possible to estimate the total force transmitted to the housing. According to the geometry of the bearing and its operating conditions (ie. shaft angular speed), the FFT that the forces transmitted is univocal (Fig.6).

The response of each type of defect has its own frequency structure, i.e. the spectra of the responses to a pit on the fixed (outer) race is completely different from the spectra of the responses to a pit on the rotating (inner) race as well as from the spectra of responses to cage wear. Looking at Fig.6, if the pit is on the fixed ring (outer race), the reaction forces spectra exhibits harmonics at the Ball Pass Frequency of the Outer race (BPFO) and at its multiples.

Alternatively, if the pit is on the rotating ring (inner race), the reaction forces spectra is more complicated due to the interactions of bearing elements; in particular, there are harmonics at the Ball Pass Frequency of the Inner race (BPMF), surrounded by side bands, evenly spaced, of the rotating ring speed.

**Case study**

The parametric model described in the paper has been used to simulate failures on the bearing of a real mechanical transmission installed on a rolling mill.

The layout of the transmission to be analysed is depicted in Fig. 7. The transmission is used in a rolling mill plant and it has a speed ratio of 0.072. Shaft 0 is connected to the motor, while shafts 2 and 3 are linked by spindles to the rolls of the mill. Speed reduction is obtained from the first two stages of the transmission, while the third one (whose ratio is equal to 1) is used to split the power to the two rolling rolls. Bearings configuration is resumed in Table 1. According to different operating conditions and different kinds of defects, the model can evaluate the forces applied to the chassis along X and Y directions.

Because of the complexity of the system and the wide variation of the frequency response, due to the mounting and assembling operation, as well as to manufacturing tolerances, the relationship between forces applied on the housing, and the corresponding virtual accelerations, is obtained experimentally.

The frequency response function between the force exerted on the chassis and the corresponding acceleration can be obtained with impulsive tests. Fig. 8 shows, as an example, the frequency response function between the force exerted on the chassis along the X axis near the bearing B1, and the acceleration measured along the same direction.

Once the forces transmitted to the chassis, due to a defective bearing, are identified from the mathematical model, the corresponding accelerations can be easily obtained by simply multiplying the forces (in frequency domain) to the frequency response functions of the

system. As an example, let's consider bearing B1. The acceleration along the X axis  $x''_{B1}(f)$  can be computed by multiplying the frequency response function of the chassis, close to bearing B1,  $TF_{x,B1}(f)$  and the force ( $F_{x,B1}(f)$ ) along the same direction estimated by the model for a defect on bearing B1.

Figs. 9, 10 and 11 respectively show the quantitative estimation of the forces applied along X direction and the corresponding accelerations for different kinds of defects. Numerical analysis has been carried out considering motor torque:  $T_M=14kN$ , motor angular speed  $\omega_M=500rpm$ ,  $C_d = 0.1mm$  for defect on the outer ring,  $C_d = 0.1mm$  for defect on the inner ring,  $C_d = 3.2mm$  for defect on the cage.

**Remarks**

The response of each type of defect has its own frequency structure, i.e. the spectra of the responses to a pit on the fixed (outer) race is completely different from the spectra of responses to a pit on a rotating (inner) race as well as from the spectra of the responses to a cage wear. While the entity of the harmonics due to pits are much higher than the harmonics due to cage wear, a cage wear will be more difficult to detect, i.e. when it has reached considerable dimensions. Coming to the accelerations that may be measured on the chassis, it is worth observing that, even if the frequency structure has not changed, the harmonics distribution has been radically altered by the response of the gear box structure, which amplifies some frequency ranges and hardly smooths others.

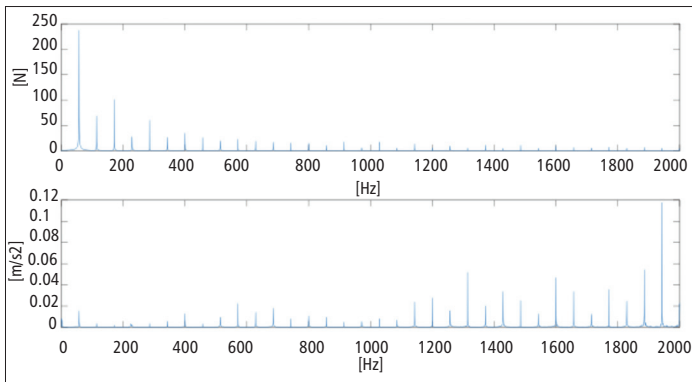


Fig 9. Forces applied on the chassis along X direction (up) and corresponding virtual acceleration (bottom) for a defect on the outer ring

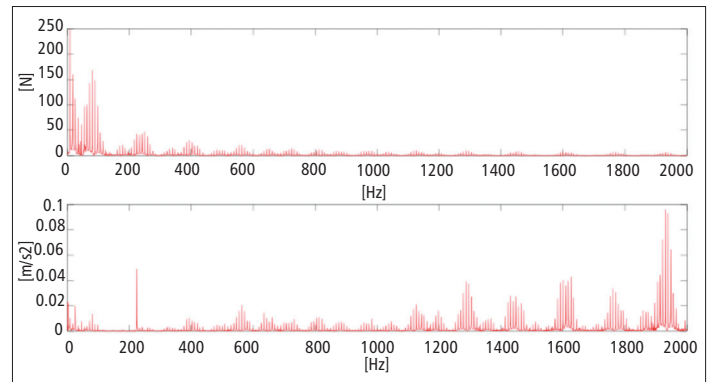


Fig 10. Forces applied on the chassis along X direction (up) and corresponding virtual acceleration (bottom) for a defect on the inner ring

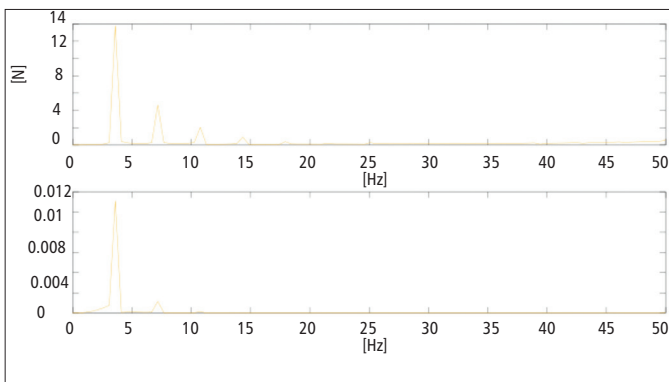
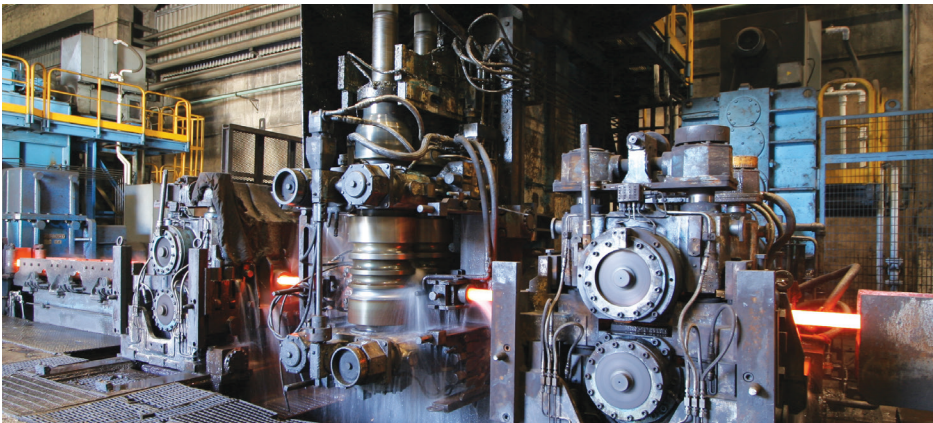


Fig 11. Forces applied on the chassis along X direction (up) and corresponding virtual acceleration (bottom) for a defect on the cage



The usefulness of the presented approach and tools, therefore, appear evident: they allow geared systems and condition monitoring developers to pre-determine system responses to defective bearings, help transmission designers to design systems where the frequency response does not transmit excessively defective bearing-exciting forces, and allows condition monitoring system developers to train and fine-tune systems aimed at detecting bearing faults. Condition monitoring system developers, for instance, may identify more clearly which frequency range has to be more accurately examined, as well as which accelerations magnitude they have to expect. The approach introduced in

this paper can significantly increase the reliability of condition monitoring systems, by making them capable of more accurately detecting incipient failures and estimating more accurately the residual life of bearings, resulting in an improvement of maintenance efficiency and effectiveness, and a reduction of running costs. ■

Further information, [www.primetals.com](http://www.primetals.com)

#### References

1. J. Antoni and R. B. Randall. A Stochastic Model for Simulation and Diagnostics of Rolling Element Bearings With Localised Faults. *Journal of Vibration and Acoustics*, 125(3):282, 2003.
2. M. Cao and J. Xiao. A comprehensive

dynamic model of double-row spherical roller bearing. **Model development and case studies** on surface defects, preloads, and radial clearance. *Mechanical Systems and Signal Processing*, 22(2):467–489, February 2008.

3. Feiyun Cong, Jin Chen, Guangming Dong, and Michael Pecht. Vibration model of rolling element bearings in a rotor-bearing system for fault diagnosis. *Journal of Sound and Vibration*, 332(8):2081–2097, April 2013.

4. Hirotohi Aramaki. Package BRAIN . (3):15–24, 1997.

5. Fucai Li, Lin Ye, Guicai Zhang, and Guang Meng. Bearing Fault Detection Using Higher-Order Statistics-Based ARMA Model. *Key Engineering Materials*, 347:271–276, 2007.

6. Robert B. Randall and J'Jerome Antoni. Rolling element bearing diagnostics – a tutorial. *Mechanical Systems and Signal Processing*, 25(2):485–520, February 2011.

7. M. Craig, T.J. Harvey, R.J.K. Wood, K. Masuda, M. Kawabata, and H.E.G. Powrie. Advanced condition monitoring of tapered roller bearings, Part 1. *Tribology International*, 42(11-12):1846–1856, December 2009.

8. S Crep, I Bercea, and N Mitu. A dynamic analysis of tapered roller bearing under fully flooded conditions. Part 1: Theoretical formulation. *Wear*, 188, 1995.

9. Suri Ganeriwala. *Rolling Element Bearing Faults*. Rolling Element Bearing Faults. 2010.

10. Janetta Culita, Dan Stefanoiu, Florin Ionescu, and Computer Science. Simulation models of defect encoding vibrations. *Control Engineering and Applied Informatics*, 9(2):59–67, 2007.

11. D. Ho and R.B. Randall. Optimisation of Bearing Diagnostic Techniques Using Simulated and Actual Bearing Fault Signals. *Mechanical Systems and Signal Processing*, 14(5):763–788, September 2000.

12. I. Bercea, S. Cretu, and D. Nelias. Analysis of Double-Row Tapered Roller Bearings, Part I - Model. *Tribology Transaction*, 46(2):11, 2003.